Assessment of high resolution centered scheme for detonation modelling

H.D. Ng†§, N. Nikiforakis‡ and J.H.S. Lee†

† Department of Mechanical Engineering, McGill University, Montreal, Canada, H3A 2K6

‡ Department of Applied Mathematics and Theoretical Physics, University of Cambridge, UK, CB3 0WA

Abstract. The present work is mainly concerned with the suitability of a high-resolution centered numerical scheme, namely the slope limiter centered scheme, in the context of simulation of detonation waves. In this paper, the results of computations with this centered scheme on a suite of one-dimensional and two-dimensional benchmark test problems are presented. It is demonstrated that the quality of the results obtained by the central differencing scheme is comparable with those of the upwind schemes at a moderate numerical resolution typically used in literature. Nevertheless, it is found that the centered scheme cannot achieve the same accuracy at coarser spatial resolutions due to its large dissipative nature. In this paper, we study a possible improvement by constructing the SLIC scheme in a multi-stage predictor-corrector fashion. It is shown that the modified k-stage SLIC scheme based on such approach can provide sufficiently accurate results for low-resolution simulations, while retaining its advantages of simplicity, robustness and generality.

§ To whom correspondence should be addressed (eddie.ng@mail.mcgill.ca)

1. Introduction

For high-speed combustion phenomena, the fluid dynamics are generally governed by a system of hyperbolic conservation laws with an addition of source terms to the governing equations for the chemistry. A variety of efficient high-resolution numerical schemes for hyperbolic systems of partial differential equations has been devised in the recent past. Many of these modern high-resolution numerical schemes are often based on *upwind* differencing, which are generally most suitable for the numerical solution of systems of hyperbolic conservation laws as they introduce characteristic information regarding the local directionality of the flow along the discontinuous interfaces of the spatial cells. Nevertheless, these upwind differencing schemes generally require the solution of the corresponding local Riemann problem to evaluate the flux terms at the cell interfaces and this in turn greatly complicates the upwind algorithm. Furthermore, the quality of the global solution depends quite crucially on the particular Riemann solver being used (Toro 2003). It sometimes lacks of generality in a sense that small modifications of the physics of a model can lead to major changes in the implementation of higher-Godunov upwind methods and their Riemann solvers.

In contrast, it is possible to construct centered schemes, which do not require information to be provided about the Riemann problem of the evolved equations. No intricate and time-consuming Riemann solvers and related characteristic decomposition are necessary, which are the building block of the high-resolution upwind schemes. In recent years, central differencing schemes for the approximate solution of hyperbolic systems of conservation laws received a lot of attention (for instance, see Nessyahu & Tadmor 1990). The main feature of such centered schemes is simplicity: they usually have a low computational cost and do not have user-adjusted parameters. Due to their simple structure, the methods can be applied very easily to any hyperbolic system in flux-conservative form. While central schemes are usually more simple and flexible than a Riemann-solver based integration method, there is a cost of an increase in numerical diffusion. Thus, the numerical results (discontinuities and rarefraction waves) are slightly more smeared than would be expected if a Riemann-solver based method were used at a similar resolution. Nevertheless, centered schemes do not compromise the qualities of the high-resolution family, albeit at a small loss of 'sharpness' of the solution (Anile *et al.* 2000).

Due to the recent interest in the pulse detonation wave engine concept (Lynch & Edelman 1996), research in detonation physics, both experimentally and numerically, is becoming increasingly significant. Numerical simulations of detonation wave, i.e. high-speed combustion wave which consists of a shock wave traveling at supersonic velocity followed by a chemical reaction zone, deal with strong non-linear interactions between gas-dynamics and chemistry. A full understanding of these coupled phenomena thus requires reliable and highly resolved numerical simulations. As a result, these simulations are often very computationally intensive. An increasing attention is also recently devoted for the inclusion of detailed chemical kinetic mechanisms in the

simulation of multi-dimensional detonation problem. Many more complex systems are being developed to study multi-phase detonations for industrial applications as well as magnetohydrodynamics (MHD) detonations in astrophysics. For these reasons, we revisited here a centered scheme in the context of detonation simulation due to its low computational cost, ease of implementation and generality. The objective of this paper is therefore to report on the suitability of the use of a centered scheme for high-speed combustion modeling. It also forms part of a validation and assessment procedure for the developed numerical code and provides all the numerical details for our recent papers (Radulescu *et al.* 2003; Ng & Lee 2003; Ng *et al.* 2003a, Ng *et al.* 2003b). To this end, a well-established high-resolution centered scheme, namely the slope limiter centered (SLIC) scheme by Toro is considered here (see Toro 1997; Toro & Billet 2000). This particular numerical scheme has been used in other disciplines such as hydrodynamical semiconductor simulations (Anile *et al.* 2000), which also involve highly nonlinear phenomena. In the present study, the proposed centered scheme is assessed against several numerical examples of time-dependent problems as benchmark tests, including the simulations of one-dimensional pulsating instabilities of planar detonations and two-dimensional cellular detonations with simple chemistry, as well as detonation initiation by reflected shock with a realistic detailed hydrogen-oxygen-argon chemical kinetic mechanism. Finally, we discuss some possible improvements on the SLIC scheme to achieve the accuracy of the best of upwind schemes, while retaining simplicity and generality.

2. Description of the numerical method

2.1. Slope limiter centered scheme

The numerical method used here for approximating the solution of hyperbolic conservation laws employs the finite volume approach where the integral formulation of the conservation laws is discretized directly in the physical space. For a 1-D system of partial differential equations written in conservative form, this can be expressed as

$$\frac{\partial \mathbf{U}}{\partial t} + \frac{\partial \mathbf{F}\left(\mathbf{U}\right)}{\partial x} = 0 \tag{1}$$

where $\mathbf{U}$ is the vector of conserved variables and $\mathbf{F}(\mathbf{U})$ the convective fluxes. The resulting update finite volume formula derived by considering the equivalent integral formulation,

$$\oint \left[\mathbf{U}dx + \mathbf{F}\left(\mathbf{U}\right)dt\right] = 0 \tag{2}$$

can be written as:

$$\mathbf{U}_i^{n+1} = \mathbf{U}_i^n + \frac{\Delta t}{\Delta x}\left[\mathbf{F}_{i-1/2} - \mathbf{F}_{i+1/2}\right] \tag{3}$$

where $\mathbf{U}_i^{n+1}$ and $\mathbf{U}_i^n$ are the conserved variables at the next and current time-levels, $n+1$ and n, respectively. $\mathbf{F}_{i-1/2}$ and $\mathbf{F}_{i+1/2}$ are the numerical fluxes at the interfaces of the computational cells of the discretized space. For a known value of Δx (based on the

desired resolution) and Δt (based on CFL stability criterion), we can advance the vector of conserved variables $\mathbf{U}$, from time level t^n to t^{n+1} if the fluxes are known. To this end the centered scheme uses a nonlinear combination of a good second (or higher)-order scheme with a first-order monotone scheme.

The slope limiter centered scheme described here is a combination of the second-order MUSCL-Hancock and the first-order centered (FORCE) scheme (see Toro 1997; Toro & Billet 2000). In the MUSCL-Hancock approach, a second-order scheme can be achieved by reconstructing the data as piecewise linear function in every cell. Such a modification gives the boundary extrapolated values for cell i

$$\mathbf{U}_i^L = \mathbf{U}_i^n - \frac{1}{2}\mathbf{\Delta}_i, \qquad \mathbf{U}_i^R = \mathbf{U}_i^n + \frac{1}{2}\mathbf{\Delta}_i \tag{4}$$

where $\mathbf{\Delta}$ is a slope vector. These new boundary values are then evolved in time by half a time-step using the usual conservative formula

$$\bar{\mathbf{U}}_i^L = \mathbf{U}_i^L + \frac{1}{2}\frac{\Delta t}{\Delta x}\left[\mathbf{F}(\mathbf{U}_i^L) - \mathbf{F}(\mathbf{U}_i^R)\right], \bar{\mathbf{U}}_i^R = \mathbf{U}_i^R + \frac{1}{2}\frac{\Delta t}{\Delta x}\left[\mathbf{F}(\mathbf{U}_i^L) - \mathbf{F}(\mathbf{U}_i^R)\right] \tag{5}$$

Instead of relying on the solution of the Riemann problem, the inter-cell numerical fluxes in the finite volume formula (equation (3)) are evaluated using the first-order centered (FORCE) scheme, which is a combination of the first-order Lax-Friedrichs and second-order Richtmyer fluxes

$$\mathbf{F}_{i+1/2}^{force} = \mathbf{F}_{i+1/2}^{force}(\bar{\mathbf{U}}_i^R, \bar{\mathbf{U}}_{i+1}^L) = 0.5\left[\mathbf{F}_{i+1/2}^{LF}(\bar{\mathbf{U}}_i^R, \bar{\mathbf{U}}_{i+1}^L) + \mathbf{F}_{i+1/2}^{Ri}(\bar{\mathbf{U}}_i^R, \bar{\mathbf{U}}_{i+1}^L)\right] \tag{6}$$

where the first-order Lax-Friedrichs flux $\mathbf{F}^{LF}$ is given by:

$$\mathbf{F}_{i+1/2}^{LF} = \mathbf{F}_{i+1/2}^{LF}(\bar{\mathbf{U}}_i^R, \bar{\mathbf{U}}_{i+1}^L) = 0.5\left[\mathbf{F}(\bar{\mathbf{U}}_i^R) + \mathbf{F}(\bar{\mathbf{U}}_{i+1}^L)\right] + 0.5\frac{\Delta x}{\Delta t}\left[\bar{\mathbf{U}}_i^R - \bar{\mathbf{U}}_{i+1}^L\right] \tag{7}$$

and the second-order Richtmyer flux $\mathbf{F}^{Ri}$ is found by first evaluating an intermediate state $\mathbf{U}^{Ri}$

$$\mathbf{U}_{i+1/2}^{Ri} = \mathbf{U}_{i+1/2}^{Ri}(\bar{\mathbf{U}}_i^R, \bar{\mathbf{U}}_{i+1}^L) = 0.5\left[\bar{\mathbf{U}}_i^R + \bar{\mathbf{U}}_{i+1}^L\right] + 0.5\frac{\Delta t}{\Delta x}\left[\mathbf{F}(\bar{\mathbf{U}}_i^R) - \mathbf{F}(\bar{\mathbf{U}}_{i+1}^L)\right] \tag{8}$$

which is then used to compute $\mathbf{F}_{i+1/2}^{Ri} = \mathbf{F}^{Ri}(\mathbf{U}_{i+1/2}^{Ri})$. The resulting numerical scheme is second-order accurate in space and time. So to avoid spurious oscillations in the vicinity of steep gradients, the slope $\mathbf{\Delta}$ is "limited" using a slope limiter function. The solution is then updated by evaluating the conservative finite volume formula (equation (3)). For further details on this high-resolution non-oscillatory centered scheme, as well as different slope limiter function and validation problems for non-reactive compressible flow, see the textbook by Toro (1997).

2.2. Method of fractional steps

The governing equations for the chemically reactive flow problem are generally of the form:

$$\frac{\partial \mathbf{U}}{\partial t} + \frac{\partial \mathbf{F}(\mathbf{U})}{\partial x} = \mathbf{S}(\mathbf{U}) \tag{9}$$

where an additional source term $\mathbf{S}(\mathbf{U})$ appears in the formulation in order to model the chemical energy release from the reactions. We therefore adopt the method of fractional steps for the numerical integration to treat separately the hydrodynamics process and the chemical reaction process, where the homogeneous hyperbolic part of (equation (9))

$$\frac{\partial \mathbf{U}}{\partial t} + \frac{\partial \mathbf{F}(\mathbf{U})}{\partial x} = 0 \tag{10}$$

is first solved by using the SLIC scheme (with initial and boundary conditions as specified for the complete system). The remaining ordinary differential equations describing the chemical reactions

$$\frac{d\mathbf{U}}{dt} = \mathbf{S}(\mathbf{U}) \tag{11}$$

are then integrated implicitly using conventional techniques. To maintain second-order accuracy, the Strang splitting method (Strang 1964) is used with the following algorithm:

$$\mathbf{U}_i^{n+1} = L_C^{\Delta t/2} L_S^{\Delta t} L_C^{\Delta t/2} \mathbf{U}_i^n \tag{12}$$

where L_C and L_S denote the operator for the convective and reactive source terms, respectively.

3. Time-dependent detonations with simplified single-step chemistry

3.1. One-dimensional pulsating detonation instabilities

Detonation phenomenon has been a subject of intense theoretical and computational studies for a long time, beginning with the earlier classical theory by Chapman-Jouguet (C-J theory) for determining the unique detonation velocity corresponded to the combustible mixture. In the 1940s, Zeldovich, von Neumann and Döring independently proposed a model for the structure of a detonation wave (see Fickett & Davis 1979). This classical model for the detonation structure, which has come to be referred as the ZND model, consists of a steady "laminar" detonation structure where a leading shock triggers the chemical reaction by adiabatic shock compression. This simple one-dimensional description still retains many of the essential physical phenomena associated with detonations. In addition, the ZND detonation structure and instabilities associated with this one-dimensional representation are mostly used as the canonical problem against which numerical schemes are validated (Hwang *et al.* 2000).

Experimentally, it is well-known that all real detonations are unstable and have a complicated three-dimensional structure. Instabilities associated with the one-dimensional planar ZND structure have been revealed by Erpenbeck (1962, 1964) via a linear stability analysis. The non-linear intrinsic oscillatory behavior of one-dimensional detonations with simple chemistry has also been shown numerically by Fickett & Wood (1966) using the method of characteristics. Since then, more thorough studies on one-dimensional pulsating detonations have been carried out by numerous researchers (see, for example, Bourlioux *et al.* 1991; He & Lee 1996; Sharpe & Falle 1999; etc.). Because of the extensive numerical examination of this canonical 1-D unsteady detonation

problem over the past, it is used widely as a benchmark problem for high-resolution numerical schemes for detonation simulations. Therefore, we will first use this problem to evaluate the performance of the described SLIC method together with the operator splitting for combustion driven flow. The propagation of detonation wave with a single-step, irreversible chemical reaction can be modeled by the Euler equations coupled with a species equation. In one space dimension, the governing equations can be written in non-dimensional form as

$$\frac{\partial \mathbf{U}}{\partial t} + \frac{\partial \mathbf{F}(\mathbf{U})}{\partial x} = \mathbf{S}(\mathbf{U}) \tag{13}$$

where the conserved variable $\mathbf{U}$, the convective flux $\mathbf{F}$ and reactive source term $\mathbf{S}$ are, respectively,

$$\mathbf{U} = \begin{pmatrix} \rho \\ \rho u \\ E \\ \rho\lambda \end{pmatrix} \qquad \mathbf{F}(\mathbf{U}) = \begin{pmatrix} \rho u \\ \rho u^2 + p \\ (E+p)\,u \\ \rho u \lambda \end{pmatrix} \qquad \mathbf{S}(\mathbf{U}) = \begin{pmatrix} 0 \\ 0 \\ 0 \\ \dot{w} \end{pmatrix} \tag{14}$$

with

$$E = \frac{p}{(\gamma - 1)} + \frac{\rho u^2}{2} + \rho\lambda Q \tag{15}$$

$$T = \frac{p}{\rho} \tag{16}$$

$$\dot{w} = -k\rho\lambda \exp\left(\frac{-E_a}{T}\right) \tag{17}$$

In the above equations, ρ, u, p, T and E are density, particle velocity, pressure, temperature and total energy per unit volume, respectively. The variable λ is the reaction progress variable, which varies between 1 (for unburned reactant) and 0 (for product). The mixture is assumed to be ideal and calorically perfect (with constant specific heat ratio γ). The parameter Q and E_a represent the non-dimensional heat release and activation energy, respectively. These variables have been made dimensionless with reference to the uniform unburned state ahead of the detonation front. The pre-exponential factor k is an arbitrary parameter that merely defines the spatial and temporal scales. It is chosen such that the half-reaction length $L_{1/2}$, i.e. the distance required for half the reactant to be consumed in the steady ZND wave, is scaled to unit length. The simulations were always initialized by imposing the corresponding steady ZND solution onto the computational grids. In the present study of instabilities of 1-D unsteady detonations, we follow Bourlioux *et al.*(1991) and fix the dimensionless parameters with the values $Q = 50, \gamma = 1.2, E_a = 50$ and overdriven factor $f = 1.6$ (i.e. $f = (D/D_{CJ})^2$ where D is the detonation velocity of the equivalent steady ZND detonation and D_{CJ} is the minimum Chapman-Jouguet detonation velocity) so that detailed comparison can be made. According to a number of linear stability analysis (Bourlioux *et al.*1991; Lee & Stewart 1991), the corresponding ZND profile has a single instability mode. Various numerical computations also show that the nonlinear

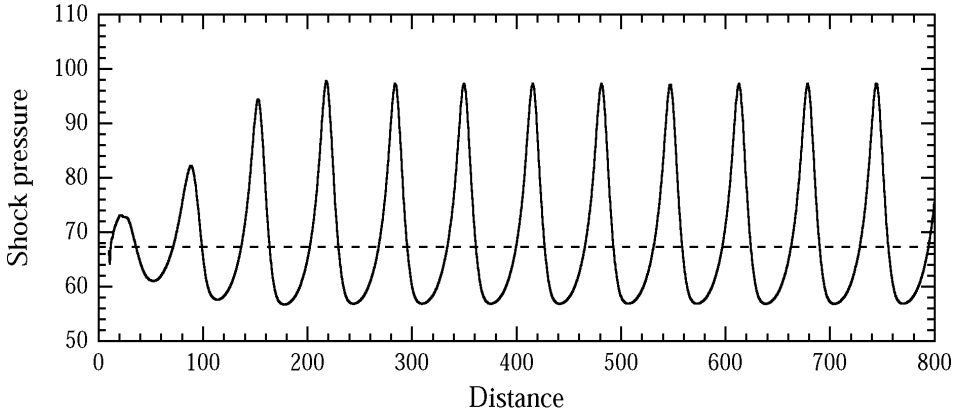

Figure 1. Pressure behind the shock front versus position for the overdriven detonation with $Q = 50$, $\gamma = 1.2$, $E_a = 50$ and $f = 1.6$, using 20 grid points per $L_{1/2}$. The dashed line indicates the steady-state ZND value of the von Neumann pressure P_{VN}.

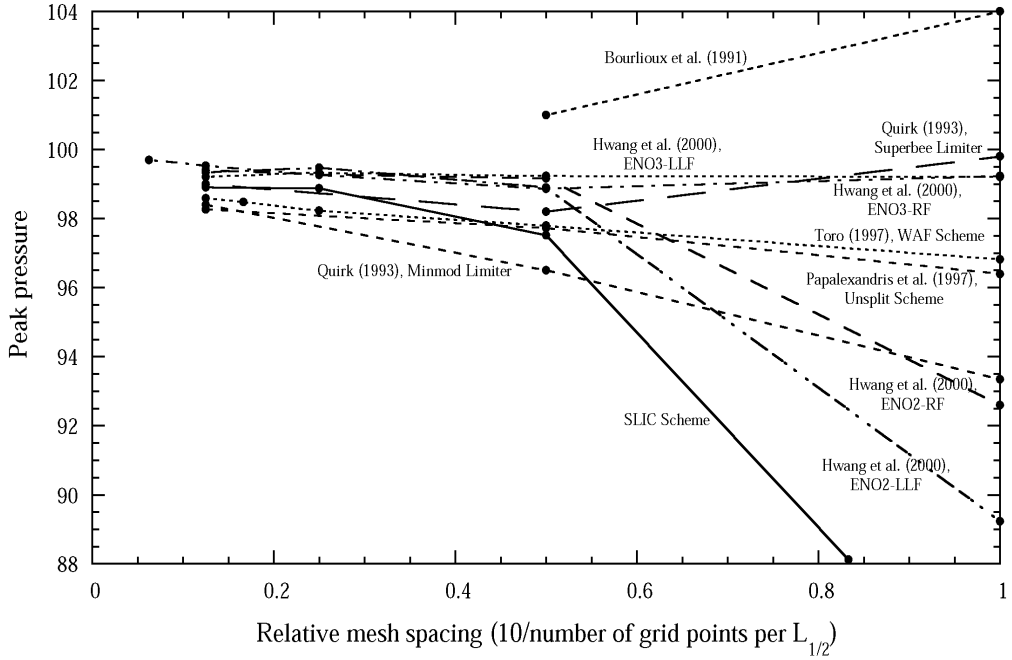

Figure 2. Comparisons of peak pressure behind the shock front as a function of relative mesh spacing among different numerical schemes for the overdriven pulsating detonation ($Q = 50$, $\gamma = 1.2$, $E_a = 50$ and $f = 1.6$).

manifestation of this instability is a regular periodic pulsating detonation (Bourlioux *et al.*1991; He & Lee 1996; etc.). Figure 1 shows the leading shock pressure versus position plot generated using the SLIC scheme. Note that there is no perturbation applied to the ZND initial condition but the instability grows quickly from the numerical startup error. After the transient development, it correctly predicts the single instability mode of the detonation front.

Following the work by Hwang *et al.* (2000), a convergence study for the peak

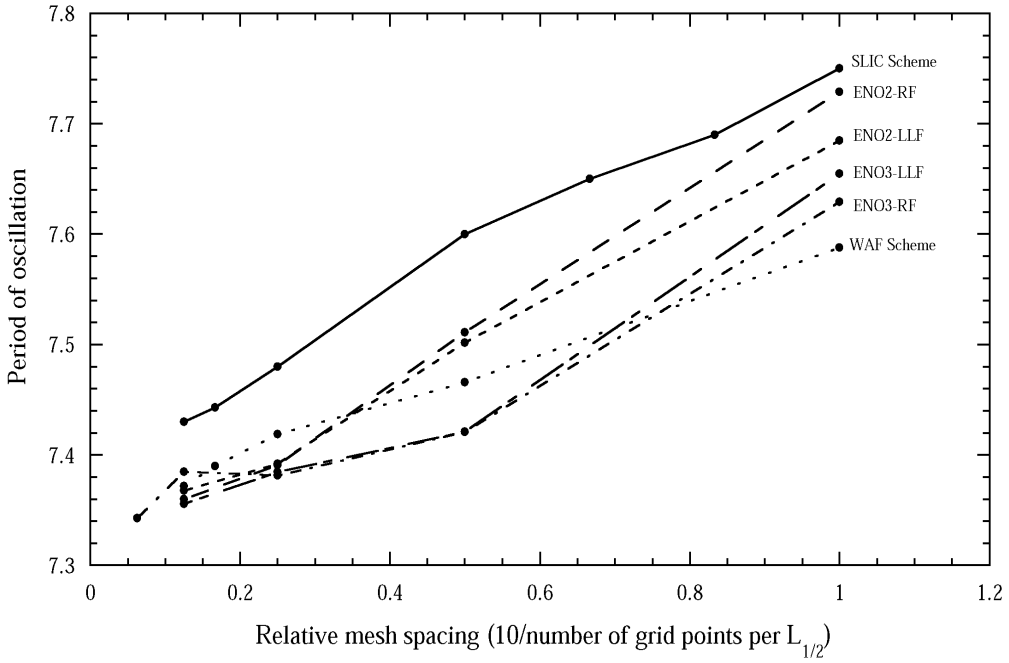

Figure 3. Comparisons of the period of pressure oscillation as a function of relative mesh spacing obtained by different ENO schemes (Hwang *et al.* 2000), the WAF scheme (Toro 1997) and the present SLIC scheme for the overdriven pulsating detonation ($Q = 50$, $\gamma = 1.2$, $E_a = 50$ and $f = 1.6$).

pressure magnitude behind the overdriven detonation reached during the limit-cycle pulsations is performed. The present results are compared with those obtained previously from various numerical schemes (Bourlioux *et al.* 1991; Quirk 1994; Papalexandris *et al.* 1997; Hwang *et al.* 2000; Toro 1997) and they are presented in Figure 2, showing the peak shock pressure vs. the relative mesh spacing (i.e., a relative mesh spacing of 0.5 corresponds to a resolution of 20 grid points per $L_{1/2}$). From this graph, we can see that the SLIC scheme, like the other schemes, converges to approximately the peak pressure value of ~ 98.6 as first predicted by Fickett & Wood (1966). Nevertheless, one may notice that the SLIC scheme approaches the correct value at a slightly higher resolution compared to other Riemann-solver based methods. At low resolution (less than 20 cells per $L_{1/2}$), the SLIC method is less accurate. This is to be expected because the SLIC method is more diffusive than Riemann-solver based method and the numerical results are slightly more smeared. Since the effects of numerical diffusion are decreased as the solution resolution increases, therefore, higher resolution for SLIC is generally necessary to accurately converge to the solution than would be expected if a Riemann-solver based methods were used.

Beside the convergence in peak pressure, it is also important to consider the period of oscillation for the pulsating detonations (see Hwang *et al.* 2000). Figure 3 compares the period of pressure oscillation with the relative mesh spacing obtained by the SLIC scheme as well as different ENO (Essentially Non-Oscillating) schemes used by Hwang *et al.* (2000). The period of oscillation is determined by taking the average of several

cycles between successive pressure peaks. The results show that the present SLIC scheme converges to a period in the range 7.4-7.5 at high resolutions. These are comparable with the non-linear stability analysis by Erpenbeck (1967), which predicted a period of 7.41-7.49. However, it is interesting to note that the converged value is slightly different to that obtained by different ENO schemes, which indicates that the predicted period depends on the numerical schemes. Overall, it is found recently by Hwang *et al.* (2000), that a reaction zone resolution of at least 20 points per $L_{1/2}$ is usually required for accurate resolution of the detonation wave with an overdrive of $f = 1.6$ if an upwind numerical scheme is used. Similar conclusion can be made here using the SLIC scheme. Above this numerical resolution, both centered and upwind achieve the same accuracy.

3.2. Two-dimensional cellular detonation simulations

Multi-dimensional detonation waves generally exhibit a complex and unsteady reaction zone structure. Two-dimensional detonation waves are characterized by an ensemble of interacting transverse waves sweeping laterally across the leading shock front of the detonation wave, see Fickett & Davis (1979). The interaction of incident shocks, Mach stems and transverse waves form a characteristic cellular pattern, producing so-called detonation cells. In the present study, we also conducted two-dimensional simulations to validate the present SLIC scheme. In 2-D case, the reactive Euler equations (equations (13) - (17)) extends to the form:

$$\frac{\partial \mathbf{U}}{\partial t} + \frac{\partial \mathbf{F}(\mathbf{U})}{\partial x} + \frac{\partial \mathbf{G}(\mathbf{U})}{\partial y} = \mathbf{S}(\mathbf{U}) \tag{18}$$

$$\mathbf{U} = \begin{pmatrix} \rho \\ \rho u \\ \rho v \\ E \\ \rho\lambda \end{pmatrix} \quad \mathbf{F}(\mathbf{U}) = \begin{pmatrix} \rho u \\ \rho u^2 + p \\ \rho uv \\ (E+p)\,u \\ \rho u\lambda \end{pmatrix} \quad \mathbf{G}(\mathbf{U}) = \begin{pmatrix} \rho v \\ \rho uv \\ \rho v^2 + p \\ (E+p)\,v \\ \rho v\lambda \end{pmatrix} \quad \mathbf{S}(\mathbf{U}) = \begin{pmatrix} 0 \\ 0 \\ 0 \\ 0 \\ \dot{w} \end{pmatrix} \tag{19}$$

$$E = \frac{p}{(\gamma - 1)} + \frac{\rho(u^2 + v^2)}{2} + \rho\lambda Q \tag{20}$$

where an additional convective flux term $\mathbf{G}$ and velocity component v are included for the transverse direction. Analogously to the fractional step operator splitting approach, one can obtain a second-order splitting scheme as follows:

$$\mathbf{U}_i^{n+1} = L_{C_X}^{\Delta t/2} L_{C_Y}^{\Delta t/2} L_S^{\Delta t} L_{C_Y}^{\Delta t/2} L_{C_X}^{\Delta t/2} \mathbf{U}_i^n \tag{21}$$

where the convective operators L_{C_X} and L_{C_Y} were of the same form as the one-dimensional convective vector in equation (10), and integrated with the same one-dimensional flow solver. For meaningful comparison, we perform the test problem considered in prior studies (Bourlioux & Madja 1992; Helzel 2000; Quirk 1994) with parameter set to $Q = 50$, $\gamma = 1.2$, $E_a = 10$ and $f = 1.2$. This corresponds to the case of high energy release and low activation energy, producing a regular cell pattern with

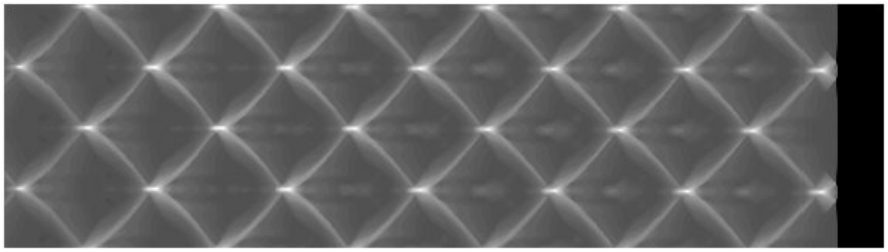

Figure 4. Numerical smoked foil record for the overdriven detonation with $Q = 50$, $\gamma = 1.2$, $E_a = 10$ and $f = 1.2$, using 24 grid points per $L_{1/2}$ and channel width = 10 half reaction lengths (shown twice).

a complex structure of transverse waves. The same degree of numerical resolution as Bourlioux & Madja (1992), i.e. 24 cells per $L_{1/2}$, is used in the present study so that direct comparison can be made. We impose the solution for the planar steady ZND wave as initial data and perturbed the wave by introducing a small curvature into the front to accelerate the growth of transverse instability. The width of the computational domain is 10 half-reaction zone lengths. Periodic boundary conditions are used along the top and bottom boundaries.

The cellular pattern so obtained is shown in Figure 4. This is a typical "numerical smoked foil" showing the time-integrated maximum pressure contour from the numerical simulation, which corresponds to the trajectories of the triple shock interactions (i.e. triple point). The obtained transverse characteristic length scale, so-called the cell size, is in agreement with that found in other published literature, which has a value of 10 for the given channel width. To look at the flow field behind the detonation front in more detail, Figures 5 show a sequence of Schlerien-type or gradient plots of pressure and density. They are very similar to Bourlioux's results and most of the characteristics of the flow field can be correctly resolved. More importantly, these results indicate the capability of the present computational method for producing highly complex simulation of multi-dimensional detonation cell phenomena. Nevertheless, it is worth noting that to resolve all the various length scales involved in the problem, a higher resolution than the one used here is indeed required as pointed out in the paper by Sharpe (2001).

4. Time-dependent detonations with realistic chemistry

So far, the numerical scheme is assessed against one and two-dimensional time-dependent detonations with only simple one-step Arrhenius chemistry. In this section, we extend the numerical scheme to include multi-species and perform simulations to validate the SLIC method coupled with detailed realistic chemistry. To include detailed chemistry, the one-dimensional Euler equations (equations (13) -(16)) can be modified to account for compressible flows with more than one species, which become:

$$\frac{\partial \mathbf{U}}{\partial t} + \frac{\partial \mathbf{F}(\mathbf{U})}{\partial x} = \mathbf{S}(\mathbf{U}) \tag{22}$$

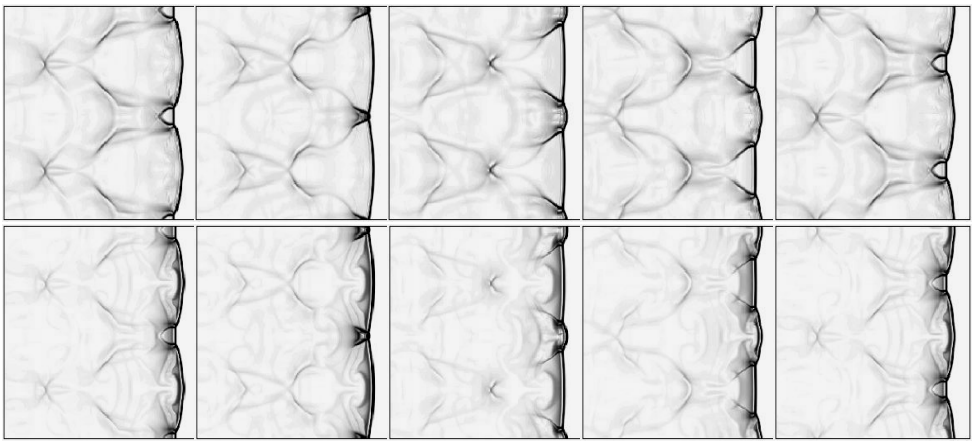

Figure 5. Sequence of five Schlieren-type plots showing the pressure (top) and density (bottom) flow field behind the shock for the overdriven detonation with $Q = 50$, $\gamma = 1.2$, $E_a = 10$ and $f = 1.2$, using 24 grid points per $L_{1/2}$ and channel width = 10 half reaction lengths (shown twice).

$$\mathbf{U} = \begin{pmatrix} \rho_1 \\ \vdots \\ \rho_{N_s} \\ \rho u \\ E \end{pmatrix} \quad \mathbf{F}(\mathbf{U}) = \begin{pmatrix} \rho_1 u \\ \vdots \\ \rho_{N_s} u \\ \rho u^2 + p \\ (E+p)\,u \end{pmatrix} \quad \mathbf{S}(\mathbf{U}) = \begin{pmatrix} \dot{w}_1 \\ \vdots \\ \dot{w}_{N_s} \\ 0 \\ 0 \end{pmatrix} \tag{23}$$

where N_s is the total number of species being considered and ρ_i are the density of the i^{th} chemical species. The total density of the gas mixture ρ is therefore given by:

$$\rho = \sum_{i=1}^{N_s} \rho_i \tag{24}$$

The total energy per unit volume for the gas mixture is designated by E, which can be written as

$$E = \rho e + \frac{\rho u^2}{2} \tag{25}$$

where e is the internal energy per unit mass of the mixture and is calculated based on a mass-weighted average of the internal energy per unit mass of each species e_i

$$e = \sum_{i=1}^{N_s} y_i e_i \tag{26}$$

where $y_i = \rho_i/\rho$ is the mass fraction of i^{th} species. For a mixture of perfect gases, each gas species has its partial pressure p_i and the equation of state for multi-species flow is therefore written as:

$$p = \sum_{i=1}^{N_s} p_i = \rho R_u T \sum_{i=1}^{N_s} \frac{y_i}{M_i} \tag{27}$$

where $R_u = 8.314\text{J/mol°K}$ is the universal gas constant and M_i is the molecular weight of the i^{th} species. In addition, the internal energy, enthalpy, and specific heats are

functions of the temperature only. Here, all gaseous species are also assumed to be thermally perfect of which the specific heats are non-constant functions of temperature. In this case, the enthalpy of each species is given by:

$$h_i(T) = h_i^f + \int_0^T c_{p_i}(T)\, dT \tag{28}$$

where $h_i^f = h_i(0)$ is the heat of formation and $c_{p_i}(T)$ is the specific heats at constant pressure of the i^{th} species, which are generally tabulated as a function of temperature for many gases. Using the following thermodynamic relation:

$$e = h - \frac{p}{\rho} = \sum_{i=1}^{N_s} y_i h_i(T) - \frac{p}{\rho} = \sum_{i=1}^{N_s} y_i h_i^f + \int_0^T \sum_{i=1}^{N_s} y_i c_{p_i}(T) dT - \frac{p}{\rho} \tag{29}$$

and the ideal gas equation of state, we can rewrite the total energy per unit volume for the gas mixture as:

$$E = \sum_{i=1}^{N_s} \rho_i h_i(T) - R_u T \sum_{i=1}^{N_s} \frac{\rho_i}{M_i} + \frac{\rho u^2}{2} \tag{30}$$

which gives an implicit relation for determining the temperature T from the conserved variable, but requiring an iteration procedure.

For the chemical kinetic model, the mass production/destruction rate of i^{th} species due to chemical reaction is represented by $\dot{w}_i$, generally derived from a given detailed chemical reaction mechanism of elementary reactions, having the form:

$$\sum_{i=1}^{N_s} \nu'_{ij} X_i \Leftrightarrow \sum_{i=1}^{N_s} \nu''_{ij} X_i \qquad j = 1, ..., N_{reac} \tag{31}$$

where ν'_{ij} and ν''_{ij} are respectively the forward and backward stochiometric coefficients of species X_i in the j^{th} reaction. N_{reac} is the total number of chemical reactions in the mechanism. Subsequently, the net mass production rate of species i can be expressed by:

$$w_i = M_i \sum_{j=1}^{N_{reac}} \left(\nu''_{ij} - \nu'_{ij}\right) q_j \tag{32}$$

where q_j is the net rate of progress for reaction j and can be written as:

$$q_j = k_j^f \prod_{i=1}^{N_s} [X_i]^{\nu'_{ij}} - k_j^b \prod_{i=1}^{N_s} [X_i]^{\nu''_{ij}} \tag{33}$$

where k_j^f and k_j^b are respectively the forward and backward reaction rate constant for reaction j. $[X_i]$ is the mole concentration of species i. The forward rate coefficients is generally given by the Arrhenius form:

$$k_j^f(T) = A_{f_j} T^{\beta_j} \exp\left(\frac{-E_{a_j}}{R_u T}\right) \tag{34}$$

with the pre-exponential constant A_{f_j}, the temperature exponent β and activation energy E_{a_j}. Knowing the forward reaction rate, the corresponding backward rate can be found by chemical equilibrium consideration and calculated by:

$$k_j^b(T) = \frac{k_j^f(T)}{k_j^{equil.}(T)} \tag{35}$$

where the $k_j^{equil.}(T)$ is equilibrium constant based on thermodynamic calculation. In this work, the rate $\dot{w}_i$ as well as other thermodynamic data for each gaseous species, such as the values of the enthalpy $h_i(T)$, the specific heats $C_{p_i}(T)$ or $C_{v_i}(T)$, etc., were obtained from the CHEMKIN package (Kee *et al.* 1989). For further explanation of the governing equations and other thermodynamic relations, see the paper by Fedkiw *et al.* (1997).

4.1. Detonation initiation by reflected shock in hydrogen-oxygen-argon mixture

We look at the detonation initiation process for a hydrogen-oxygen-argon mixture due to reflection of a shock wave in a shock tube closed at one end. The initial conditions for the computations correspond to the evolution of a strong ignition case by Oran *et al.* 1984. This particular one-dimensional example has been used extensively in the past to test numerical schemes (Deiterding 2000; Im 2002; etc). and thus, data are available in the literature so that direct comparison can be made with the results obtained from the present computations. The general configuration is a shock tube of length $L = 12$ cm filled with stoichiometric hydrogen-oxygen-argon mixture of molar ratios 2:1:7. Initially, an incident shock wave is created, which propagates through the shock tube from right to left. Once the incident shock is reflected at the end wall, a detonation wave is formed by the reflected shock heating after some induction period. For the computation, the calculation is performed in cartesian geometry covered with 4800 uniform numerical cells. The hydrogen-oxygen-argon chemistry is modeled with the same 9 species and 24-steps reaction mechanism, which was developed in reference (Oran *et al.* 1982).

To look at the flow evolution for the detonation initiation after the shock reflection from the end wall, Figure 6 shows the pressure, density and temperature profiles at subsequent time interval. These transient results obtained during different stages of the initiation process, i.e. the ignition, development and final onset of detonation, are found to be in good agreement with those from the literature (Im *et al.* 2002). After its formation behind the reflected shock, the detonation wave eventually catches up and merges with the reflected shock, causing a split into 3 waves (i.e., the rarefaction, contact surface and the detonation front). Note that these different waves are clearly captured by the present numerical schemes, as shown in the density profile of Figure 6.

Figure 7 shows the trajectory of different waves in the flow field, including the position of the shock front, reaction wave, transmitted detonation and the contact discontinuity due to the merging of the shock with reaction wave. The positions of these different waves agree well with previous results. From this plot, we can find that the

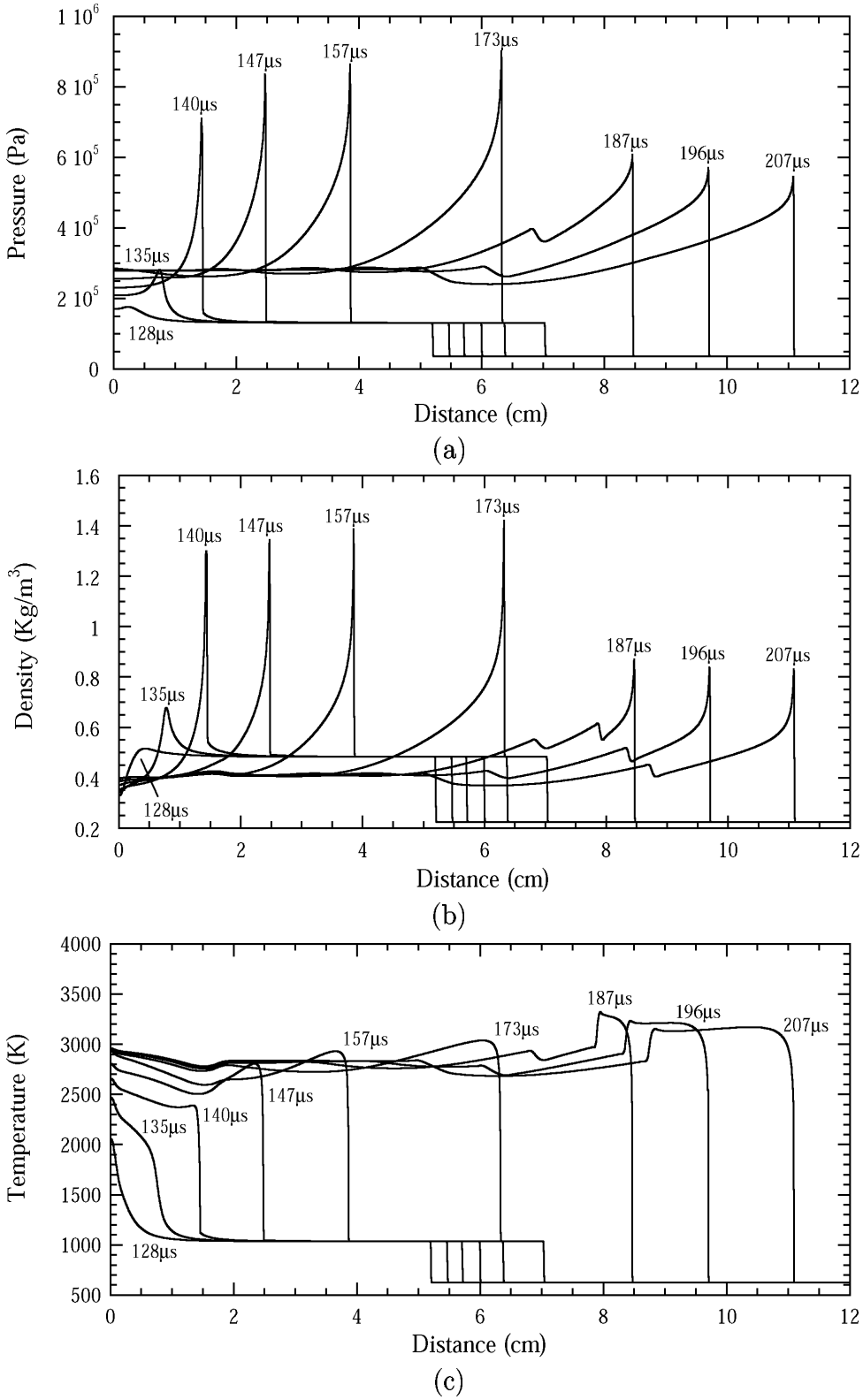

Figure 6. (*a*)Pressure, (*b*) Density and (*c*) temperature profiles showing the time evolution of the detonation intiation process by reflected shock.

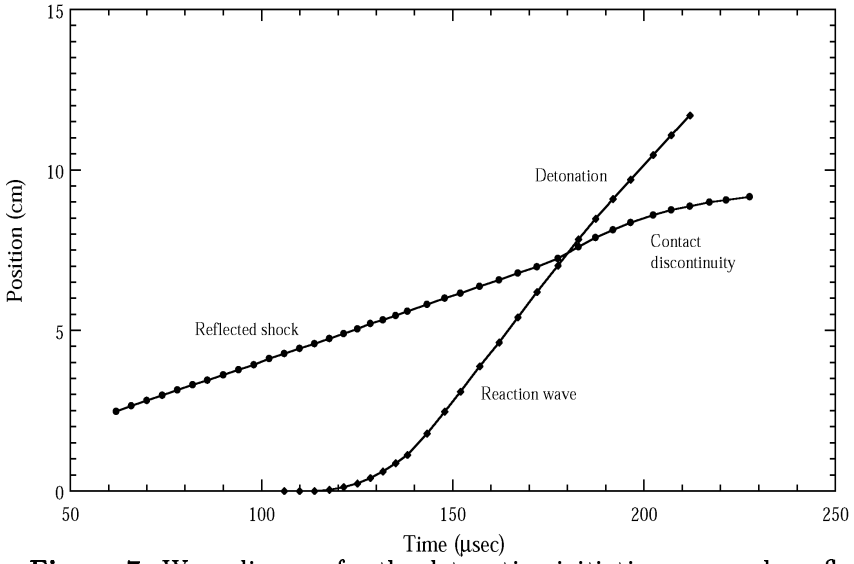

Figure 7. Wave diagram for the detonation initiation process by reflected shock.

time when the detonation and reflected shock wave merge is at a value of approximately 180μsec, which is also obtained by previous studies(Oran *et al.* 1982; Deiterding 2000; Im *et al.* 2002;). Here, comparison with previously numerical results from literatures illustrates the similar accuracy of the present approach using this SLIC scheme for the simulation with detailed chemistry.

5. An improved SLIC scheme

For moderate grid resolution, we demonstrate on several benchmark test problems that the centered SLIC method can lead to accurate approximations of detonation waves, comparable to those obtained using different best upwind schemes but has the advantage of lower computational cost and simplicity without the use of Riemann-solver. Nevertheless, in section 3.1 we have discussed that the SLIC method used in this study cannot achieve the same accuracy at coarser spatial resolutions due to large dissipative nature of the centered scheme. In this section, we study a possible way to improve the SLIC scheme for low-resolution simulations, while retaining its advantages of simplicity, robustness and generality.

A computational technique based on a multi-stage predictor-corrector approach has been recently proposed by Toro (2003) to construct numerical flux for the use in finite volume methods. The idea is that in the predictor step, a simple and robust numerical flux is used to open the Riemann fan without making use of precise knowledge of the structure of the solution of the Riemann problem. It extracts the relevant information for the corrector step, which involves the final inter-cell flux evaluation. The attractiveness of this approach is that the implementations can rely on centered fluxes at each stage. See the paper by Toro (2003) for more details. This procedure is expected to produce a numerical flux very close to that of the upwind method of Godunov scheme. Hence, the use of MUSTA approach opens up a possibility to improve existing centered scheme.

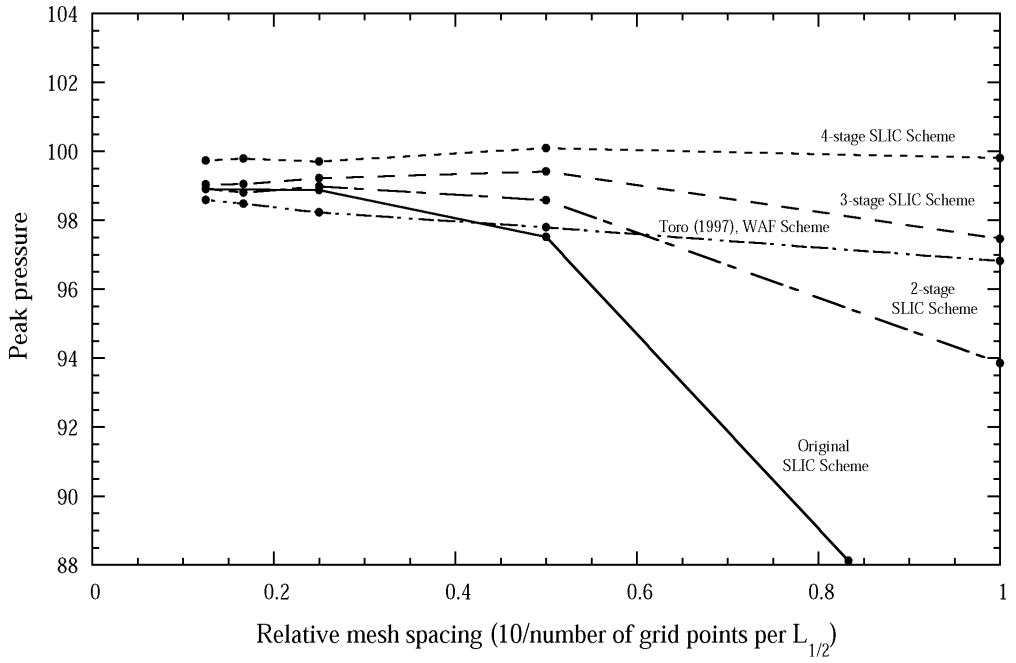

Figure 8. Comparisons of peak pressure behind the shock front as a function of relative mesh spacing between the original SLIC scheme, modified multi-stage SLIC scheme and WAF scheme for the overdriven pulsating detonation ($Q = 50$, $\gamma = 1.2$, $E_a = 50$ and $f = 1.6$).

Using the MUSTA approach, an improved SLIC scheme is obtained here by replacing the single evaluation process of the inter-cell numerical flux with a multi-stage FORCE$^{\mathrm{k}}$ scheme. It is derived by applying the centered FORCE flux described in equation (6) for both the multi-stage predictor and the corrector in the MUSTA approach (Toro 2003). By starting with $k = 1$, $\mathbf{U}_i^{(1)} = \bar{\mathbf{U}}_i^R$, $\mathbf{U}_{i+1}^{(1)} = \bar{\mathbf{U}}_{i+1}^L$, $\mathbf{F}_{i+1/2}^{\left(force^1\right)} = \left(\bar{\mathbf{U}}_i^R, \bar{\mathbf{U}}_{i+1}^L\right)$ given by equations (6) - (8), the general algorithm for the k-stage FORCE scheme is given as:

Open Riemann fan:

$$\mathbf{U}_i^{(k+1)} = \mathbf{U}_i^{(k)} - \frac{\Delta t}{\Delta x}\left[\mathbf{F}_{i+\frac{1}{2}}^{\left(force^k\right)}\left(\mathbf{U}_i^{(k)}, \mathbf{U}_{i+1}^{(k)}\right) - \mathbf{F}\left(\mathbf{U}_i^{(k)}\right)\right] \tag{36}$$

$$\mathbf{U}_{i+1}^{(k+1)} = \mathbf{U}_{i+1}^{(k)} - \frac{\Delta t}{\Delta x}\left[\mathbf{F}\left(\mathbf{U}_{i+1}^{(k)}\right) - \mathbf{F}_{i+\frac{1}{2}}^{\left(force^k\right)}\left(\mathbf{U}_i^{(k)}, \mathbf{U}_{i+1}^{(k)}\right)\right] \tag{37}$$

Flux evaluation:

$$\mathbf{F}_{i+\frac{1}{2}}^{\left(force^{k+1}\right)} = \mathbf{F}_{i+\frac{1}{2}}^{\left(force^k\right)}\left(\mathbf{U}_i^{(k+1)}, \mathbf{U}_{i+1}^{(k+1)}\right) \tag{38}$$

To illustrate the performance of the multi-stage SLIC scheme, we look at once again the canonical problem of the one-dimensional pulsating overdriven detonations considered in section 3.1. Similarly, figures 8 and 9 show the peak pressure amplitude and the period of oscillation as a function of relative mesh spacing of the overdriven detonation computed using the original SLIC scheme, the improved k-stage SLIC

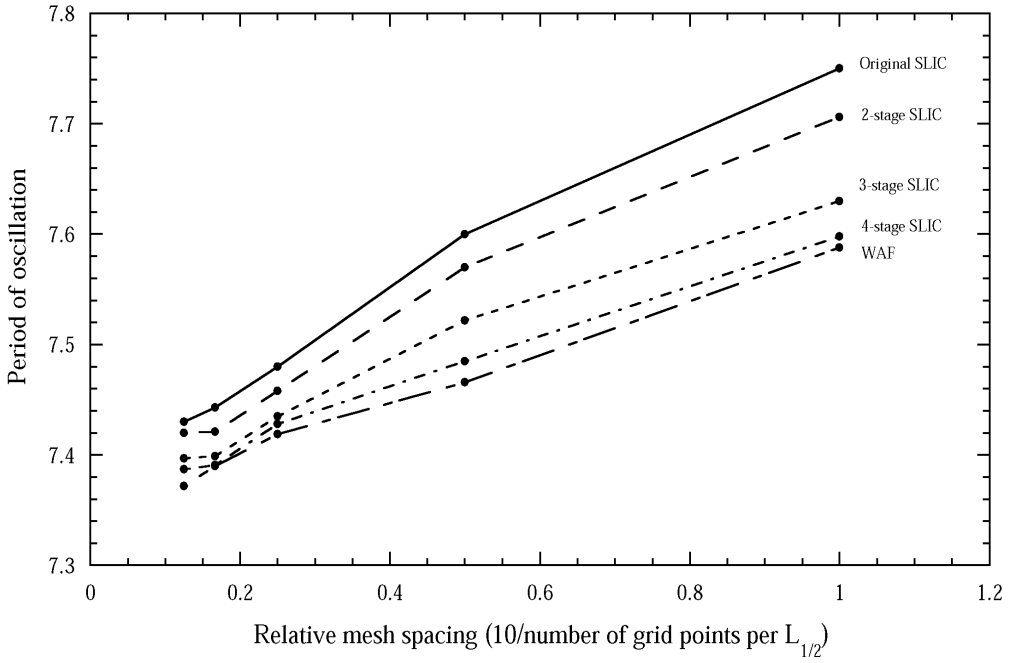

Figure 9. Comparisons of the period of pressure oscillation as a function of relative mesh spacing between the original SLIC scheme, modified multi-stage SLIC scheme and WAF scheme for the overdriven pulsating detonation ($Q = 50$, $\gamma = 1.2$, $E_a = 50$ and $f = 1.6$).

scheme (k =2, 3 and 4) and the 2$^{\text{nd}}$ order upwind WAF scheme for comparison. The improvement using the MUSTA approach can be readily shown in these plots. The multi-stage SLIC schemes are clearly able to predict more accurate results for a given mesh spacing (clearly at low resolution) than the original SLIC scheme. By increasing the number of stages in the modified SLIC scheme, the results converge faster to the correct value of peak pressure $P \sim 99$ and period of oscillations $\Omega \sim 7.4$ at coarser grid resolution. For the 3- and 4-stage SLIC schemes, they are able to approach the correct peak pressure with a relatively coarse resolution (10 points per $L_{1/2}$) and have indeed similar accuracy (or even better) to that of the upwind (WAF) method. It should be pointed out that although we can achieve better accuracy as the number of stages is increased, at the same time the computational time for evaluating the inter-cell numerical flux is also increased, which can become comparable to most existing Riemann-solver based upwind schemes. Nevertheless, the multi-stage approach retains the simplicity, robustness and generality of centered scheme. In this study, we found that the 3-stage scheme should be sufficiently accurate and is probably the preferred scheme to be used for practical high-speed flow computations.

6. Conclusion

In this paper we have presented the applicability of a high-order centered scheme, namely the SLIC scheme, for the simulation of transient detonation waves. The SLIC method

belongs to the high-resolution class of methods, which is conservative, explicit, second-order accurate in space and time. The SLIC method is 'limited' such that in the numerical solution any discontinuities are well-resolved and are not accompanied by the spurious oscillations, which occur typically for unlimited second-order schemes. In this study, we have applied this centered scheme to several canonical problems of time-dependent detonation waves with both the simple and complex chemistry. Detailed comparisons with previous published results reveal that the quality of the results obtained from this simple numerical scheme is comparable with those of the upwind schemes at typical resolution used in literature.

Our motivation to use this centered scheme comes from the fact that it does not require information about the characteristic structure of the hyperbolic equation system to be provided. Therefore, it generally has a lower computational cost and simple structure compared to most Riemann-solver based methods. However, the latter typically have the advantage when it comes to accuracy and this is more transparent for computations with coarser spatial resolution in the present study. Here, we discuss a possible way to improve the accuracy of the centered schemes using Toro's MUSTA approach. By constructing the numerical flux based on a multi-stage predictor-corrector fasion, the modified k-stage SLIC scheme achieves the accuracy of upwind methods even for low-resolution simulations but retains the simplicity and robustness of centered methods.

From the formulation of centered method, it is also apparent that once a skeleton algorithm for the scheme is coded, any system of hyperbolic conservation laws can be solved, simply by typing the corresponding vectors of the conserved variables and the numerical fluxes for the system. Indeed, this is convenient when we are solving the numerical solution of detonation wave with detailed chemistry or multi-phase components. One should also realize that the flexibility of the scheme should generalize straightforwardly to higher dimensions and also it can be incorporated easily with adaptive mesh refinement without any implementation complications.

References

Anile A M, Nikiforakis N and Pidatella R M 2000 Assessment of a high resolution centered scheme for the solution of hydrodynamical semiconductor equations *SIAM J. Sci. Comput.* **22** 1533-1548

Bourlioux A, Majda A J and Roytburd V 1991 Theoretical and numerical structure for unstable one-dimensional detonations *SIAM J. Appl. Math.* **51** 303-343

Bourlioux A and Majda A J 1992 Theoretical and numerical structure for unstable two-dimensional detonations *Combust. Flame* **90** 211-229

Deiterding R 2000 Simulation of a shock tube experiment with non-equilibrium chemistry *Technical Report, Brandenburgische Technische Universität Cottbus* **NMWR-00-3**

Erpenbeck J J 1962 Stability of steady-state equilibrium detonations *J. Phys. Fluids* **5** 604-614

Erpenbeck J J 1964 Stability of idealized one-reaction detonations *J. Phys. Fluids* **7** 684-696

Erpenbeck J J 1967 Nonlinear theory of unstable one-dimensional detonations *J. Phys. Fluids* **10** 274-288

Fedkiw R P, Merriman B and Osher S 1997 High Accuracy Numerical Methods for thermally perfect gas flows in chemistry *J. Comp. Phys.* **132** 175-190

Fickett W and Davis W C 1979 (*Detonation) (Berkeley, CA: University of California Press)*

Fickett W and Wood W W 1966 Flow calculation for pulsating one-dimensional detonations *J. Phys. Fluids* **9** 903-916

He L and Lee J H S 1995 The dynamical limit of one-dimensional detonations *J. Phys. Fluids* **7** 1151-1158

Helzel C 2000 *Numerical Approximation of Conservation Laws with Stiff Source Term for the Modelling of Detonation Waves* Thesis, Otto-von-Guericke Universität Magdeburg

Hwang P, Fedkiw R P, Merriman B, Aslam T D, Karagozian A R and Osher S J 2000 Numerical resolution of pulsating detonation waves *Combust. Theory Modelling* **4** 217-240

Im K S, Yu S T, Kim C K, Chang S C and Jorgenson P C E 2002 Application of the CESE method to detonation with realistic finite-rate chemistry *AIAA Paper, the 40th AIAA Aerospace Sciences Meeting & Exhibit, Reno, NV, Jan. 14-17* **2002-1020**

Kee R J, Rupley F M and Miller J A 1989 Chemkin-II: a Fortran chemical kinetics package for the analysis of gas-phase chemical kinetics *Sandia National Laboratories Report* **SAND89-8009**

Lee H I and Stewart D S 1990 Calculation of linear detonation instability: one-dimensional instability of planar detonations *J. Fluid Mech.* **216** 103-132

Lynch E D and Edelman R B 1996 Analysis of pulse detonation wave engine: developments in high speed vehicle propulsion systems *Prog. Astro. Aero.* **165** 473-516

Nessyahu H and Tadmor E 1990 Non-oscillatory central differencing for hyperbolic conservation laws *J. Comput. Phys.* **87** 408-463

Ng H D and Lee J H S 2003 Head-on collision of a detonation with a planar shock wave *accepted for 24th International Symposium on Shock Waves, Beijing, China*

Ng H D, Radulescu M I, Higgins A J, Nikiforakis N and Lee J H S 2003a Numerical Investigation of the instability for one-dimensional Chapman-Jouguet detonations with chain-branching kinetics *sumbitted to Combust. Theory Modelling*

Ng H D, Higgins A J, Kiyanda C B, Radulescu M I, Lee J H S, Bates K R and Nikiforakis N 2003b Nonlinear dynamics and chaos analysis on one-dimensional pulsating detonations *sumbitted to Combust. Theory Modelling*

Oran E S, Young T R, Boris J P and Cohen A 1982 Weak and strong ignition. I. Numerical simulation of shock tube experiments *Combust. Flame* **48** 135-148

Papalexandris M V, Leonard A and Dimotakis P E 1997 Unsplit schemes for hyperbolic conservation laws with source terms in one space dimension *J. Comput. Phys.* **134** 31-61

Quirk J J 1994 Godunov-type schemes applied to detonation flows *Combustion in High-Speed Flows* ed. J. Buckmaster et al., Dordrecht: Kluwer, 575-596

Radulescu M I, Ng H D, Lee J H S and Varatharajan B 2002 The effect of argon dilution on the stability of acetylene-oxygen detonations *Proc. Combust. Inst.* **29** 2825-2831

Sharpe G J and Falle S A E G 1999 One-dimensional numerical simulations of idealized detonations *Proc. R. Soc.* **455** 1203-1214

Sharpe G J 2001 Transverse waves in numerical simulations of cellular detonations *J. Fluid Mech.* **447** 31-51

Strang G 1964 Accurate partial difference methods. II. Non-linear problems *Numer. Math.* **6** 37-64

Toro E F 1997 (*Riemann Solvers and Numerical Methods for Fluid Dynamics) (Springer-Verlag, Berlin)*

Toro E F 2003 Multi-Stage Predictor-Corrector Fluxes for Hyperbolic Equations Isaac Newton Institute for Mathematical Sciences Preprint Series NI03037-NPA University of Cambridge, UK

Toro E F and Billett S J 2000 Centred TVD schemes for hyperbolic conservation laws *IMA J. Numer. Anal.* **20** 47-79